RECENT RESULTS FROM GANIL*

S. Franchoo[a], N.L. Achouri[b], A. Algora[c], A. Al-Khatib[d], J.-C. Angélique[b]
F. Azaiez[a], D. Baiborodin[e], B. Bastin[b], D. Beaumel[a], M. Belleguic[a]
G. Benzoni[f], Y. Blumenfeld[a], C. Borcea[g], R. Borcea[g], C. Bourgeois[a]
P. Bringel[d], B.A. Brown[h], A. Bürger[i], A. Buta[g], R. Chapman[j], E. Clément[k]
J.-C. Dalouzy[k], Z. Dlouhy[e], Z. Dombradi[c], A. Drouart[l], Z. Elekes[c]
C. Engelhardt[d], S. Fortier[a], Z. Fülöp[c], L. Gaudefroy[m], M. Gélin[k]
J. Gibelin[b], A. Görgen[l], S. Grévy[k], D. Guillemaud-Mueller[a], F. Hammache[a]
H. Hübel[d], S. Iacob[g], F. Ibrahim[a], K. Kemper[n], A. Kerek[o], W. Korten[l]
A. Krasznahorkay[c], K.-L. Kratz[p], B. Laurent[b], M. Lazar[g], D. Lebhertz[q]
M. Lewitowicz[k], X. Liang[j], E. Liénard[b], S. Lukyanov[r], S. Mandal[b]
C. Monrozeau[a], J. Mrazek[e], L. Nalpas[l], A. Navin[k], F. Negoita[g], F. Nowacki[q]
N. Orr[b], A. Ostrowski[p], T. Otsuka[s], D. Pantelica[g], Y. Penionzhkevich[r]
J. Piekarewicz[n], Z. Podolyak[t], E. Pollacco[l], F. Pougheon[a], A. Poves[u]
F. Rotaru[g], P. Roussel-Chomaz[k], E. Rich[a], J.-A. Scarpaci[a]
M.-G. Saint-Laurent[k], H. Savajols[k], G. Sletten[v], D. Sohler[c], O. Sorlin[k]
M. Stanoiu[g], I. Stefan[a], T. Suzuki[w], C. Theisen[l], J. Timar[c], C. Timis[g]
E. Tryggestad[a], D. Verney[a], S. Williams[t], A. Yamamoto[t]

[a]Institut de Physique Nucléaire, Orsay, France
[b]Laboratoire de Physique Corpusculaire, Caen, France
[c]Institute of Nuclear Research, Debrecen, Hungary
[d]University of Bonn, Germany
[e]Nuclear Physics Institute, Rez, Czech Republic
[f]University of Milan and INFN Milan, Italy
[g]National Institute of Physics and Nuclear Engineering, Bucharest, Romania
[h]National Superconducting Cyclotron Laboratory, East Lansing, USA
[i]University of Oslo, Norway
[j]University of the West of Scotland, Paisley, UK
[k]Grand Accélérateur National d'Ions Lourds, Caen, France
[l]CEA DSM Irfu, Gif-sur-Yvette, France
[m]CEA DAM DIF, Arpajon, France
[n]Florida State University, Tallahassee, USA
[o]Royal Institute of Technology, Stockholm, Sweden
[p]University of Mainz, Germany
[q]Institut Pluridisciplinaire Hubert Curien, Strasbourg, France
[r]Flerov Laboratory of Nuclear Reactions, Dubna, Russia
[s]University of Tokyo, Japan
[t]University of Surrey, Guildford, UK
[u]Autonomous University of Madrid, Spain
[v]Niels Bohr Institute, Copenhagen, Denmark
[w]Nihon University, Tokyo, Japan

(Received October 29, 2008)

* Presented at the Zakopane Conference on Nuclear Physics, September 1–7, 2008, Zakopane, Poland.

The shell structure of the nucleus implies the existence of magic numbers. Since several years many indications have been accumulated, theoretically as well as through experiments at various laboratories around the world, that if one moves away from stability, the location of the magic numbers shifts as an inescapable consequence of the evolving nature of the nuclear force itself. In this respect, it is the balance between the tensor and spin-orbit components that seems particularly instrumental. Illustrative examples from recent experiments at Ganil, at the neutron-rich and proton-rich side of the nuclear chart for N or Z equal 20 or 28, will be presented here.

PACS numbers: 23.20.Lv, 25.45.Hi, 25.70.–z, 27.30.+t, 27.40.+z

1. Introduction

In this paper we present some of the results obtained at the Ganil accelerator in France over the most recent years. Fragmentation, knock-out and transfer still count among the reaction mechanisms that are heavily relied upon to produce unstable nuclei and measure their properties.

For near-stable nuclei, one first comes across the magic numbers 2, 8 and 20, which belong to the harmonic oscillator potential. The next magic number is 28, the existence of which arises from the spin-orbit interaction. For neutron-rich nuclei farther from stability, the spin-orbit force could be less pronounced as the nuclear surface becomes more diffuse [1].

The tensor force, since long known to exist but seldom isolated in its proper right, has meanwhile been invoked more explicitly to explain the systematic displacement of single-particle levels throughout the nuclear chart [2]. Depending on the valence orbitals that are present, it may counteract or reinforce the spin-orbit splittings. The combined effect of the spin-orbit and tensor forces may then offer some insight into the changing shell structure that is experimentally observed in ^{20}C, ^{36}Ca, ^{42}Si, and ^{47}Ar, presented in the following paragraphs.

2. Experimental results

2.1. Carbon

The structure of neutron-rich carbon was investigated through double fragmentation combined with in-beam γ spectroscopy [3]. A ^{36}S beam at 77.5 AMeV was used to produce a cocktail beam with a transmission that was optimised for ^{24}F, ^{25,26}Ne, ^{27,28}Na, and ^{29,30}Mg. These nuclei flew at energies of 54 to 65 AMeV into an active target, consisting of a plastic scintillator sandwiched between two carbon foils of 51 mg/cm^2 each. The nuclei emerging from the reactions in the carbon foils were selected and identified in the Speg spectrometer. The 74 BaF_2 scintillators of the Château de Cristal detector array were mounted in a spherical geometry around the active target.

Doppler-corrected γ-ray spectra were obtained for ^{17,18,19,20}C. Besides other results, the energy of the 2_1^+ state was fixed at 1585(10) keV in ^{18}C and 1588(20) keV in ^{20}C. While the spectroscopy of ^{20}C was done for the first time, earlier work had located the first excited state in ^{18}C at 1620(20) keV [4].

When plotting the 2_1^+ energy systematics of the even carbon and oxygen isotopes, one observes a remarkable similarity up to $N = 12$. At $N = 14$, however, while the 2_1^+ energy in ^{20}C remains constant, in ^{22}O it jumps to 3199(8) keV [5]. In the oxygen isotopes, for a growing occupancy of the $\nu d_{5/2}$ orbital, its energy decreases relative to the $\nu s_{1/2}$ state. If this effect is ascribed to a large attractive $\nu d_{5/2}$–$\nu d_{5/2}$ two-body matrix element, it would explain the $N = 14$ subshell gap that is manifest in the 2_1^+ energy of ^{22}O. In the carbon chain, the $\nu d_{5/2}$ single-particle energy is shifted upwards with respect to $\nu s_{1/2}$. This is visible in the $1/2^+$ ground-state spin of ^{15}C [6]. USD calculations with the WBT interaction show that also here the $\nu d_{5/2}$ orbital would come down as it fills but it would not drop sufficiently below $\nu s_{1/2}$ to develop a $N = 14$ subshell gap. The near-degeneracy of both orbitals would thus explain the almost constant excitation energy of the 2_1^+ level in ^{16,18,20}C.

2.2. Calcium

One-nucleon knock-out is a reaction mechanism that has been successfully exploited at Ganil since many years. In the experiment we describe here [7], a ^{37}Ca radioactive beam at an energy of 60 AMeV was produced by fragmentation of a ^{40}Ca primary beam at 95 AMeV. A 200 mg/cm^2 thick beryllium foil provided the secondary target, yielding the desired ^{36}Ca isotope besides many side products. Identification of the heavy ejectile took place in the Speg spectrometer, while γ rays were recorded by the Château de Cristal scintillator array.

The energy of the first excited level in ^{36}Ca was determined at 3036(11) keV, consistent with the value of 3015(16) keV measured in a competing experiment at GSI [8]. This fairly high energy, some 500 keV above the proton separation energy of 2560(40) keV [9], is indicative of a subshell gap at $N = 16$. Its mirror equivalent, the 2_1^+ energy in ^{36}S, lies at 3290.9(3) keV [10]. If it would imply that the $Z = 20$ closure is maintained throughout the calcium chain, the Thomas–Ehrman shift would not be able to explain this mirror energy difference, since the 2_1^+ state in ^{36}S is well bound while the 2_1^+ state in ^{36}Ca would only have a small contribution from proton excitations.

Momentum distributions were measured in Speg for both the ground state and the 2_1^+ state. When comparing the deduced cross sections to shell-model calculations, reduction factors can be computed that give the ratio between the experimental and the theoretical spectroscopic factor [11]. For the ground state of ^{36}Ca we found a reduction that is similar to the one for

near-stable nuclei. For the 2_1^+ state, only a lower limit could be established since the possibility of proton emission could not be excluded, the detection set-up not being sensitive to it.

2.3. Silicon

The ^{42}Si isotope sits at the crossroads of $Z = 14$ and $N = 28$. It was produced by two-proton knock-out in a 195 mg/cm^2 thick beryllium target from a secondary beam of ^{44}S at 46 AMeV, the latter being the fragmentation residue of a ^{48}Ca primary beam at 60 AMeV [12]. Also here identification of the heavy ejectile relied on the Speg spectrometer and the Château de Cristal array was chosen for γ-ray detection.

The energy of the 2_1^+ state was measured at 770(19) keV. This is the lowest 2_1^+ energy at $N = 28$ and one of the smallest among nuclei of similar mass, for instance the 2_1^+ energy in ^{40}Si is situated at 986(5) keV [13]. Hence it strongly argues for the disappearance of the $N = 28$ shell gap in the silicon isotopes. This behaviour is reflected in the positions of those levels in ^{41}P and ^{43}P around 1 MeV also measured in this work that correspond to the coupling of the last proton to the 2^+ excitation of the silicon core.

Shell-model calculations for which the pf-shell neutron–neutron two-body matrix elements of the SDPF-NR interaction [14] were reduced by 300 keV give good agreement for the ^{36,38,40}Si and ^{37,39}P isotopes, but the 2_1^+ energy in ^{42}Si is predicted too high at 1.1 MeV. Modifying the proton-neutron matrix elements between $\pi d_{5/2}$ and νfp brings the energy down to 810 keV in ^{42}Si, while also for ^{41,43}P fair correspondence is reached. As a result, the $\pi d_{3/2}$–$\pi d_{5/2}$ spin-orbit splitting is reduced by 1.94 MeV from ^{34}Si to ^{42}Si. In a tensor-force picture, it can be accounted for by the filling of the $\nu f_{7/2}$ orbital onwards from ^{34}Si. The compression of the νpf single-particle energies that occurs when emptying the $\pi d_{3/2}$ and $\pi s_{1/2}$ orbitals downwards from ^{48}Ca and that decreases the $N = 28$ gap by about 1 MeV can be ascribed to the combined effect of the tensor force for $\pi d_{3/2}$ and the density dependence of the spin-orbit interaction for $\pi s_{1/2}$ [15]. The particle-hole excitations across the reduced proton and neutron shell gaps translate into a collectivity and an oblate shape for ^{42}Si with a calculated deformation of $\beta_2 = -0.45$.

2.4. Argon

Much effort is devoted at Ganil to transfer experiments. The stripping reaction ^{46}Ar$(d,p)^{47}$Ar in inverse kinematics took as objective to quantify the evolution of the $N = 28$ shell gap below ^{48}Ca [15]. The pure ^{46}Ar beam at 10 AMeV was delivered by the Spiral-1 installation at an intensity of 2×10^4 pps through the Isol technique. The beam then hit a 0.38 mg/cm^2 thick CD_2 target. The set-up included the Speg spectrometer for identification of the

outgoing heavy reaction product and the highly segmented Must-1 particle detector array at backwards angles for detection of the emitted proton.

The excitation-energy spectrum of ^{47}Ar was reconstructed, background subtracted and fitted. The mass excess was found to be $-25.20(9)$ MeV. We deduced a $N = 28$ gap of 4.47(9) MeV in ^{46}Ar, 330(90) keV less than in ^{48}Ca. DWBA angular distributions calculated with global optical potentials were fitted to the measured proton distributions. It was verified that the global optical potentials that were used, reproduce the literature data for ^{49}Ca and ^{41}Ar. The resulting level energies, transferred angular momenta, and vacancy values (defined as $(2J + 1)C^2S$, with C^2S the spectroscopic factor) were compared to shell-model calculations with the *sdpf* interaction [16]. Excitations of protons and neutrons were restricted to the *sd* and *fp* spaces, respectively. The good agreement with the experimental data allows to assign spin and parity to the lowest five levels.

In an extreme single-particle model, the total vacancy for a valence state should be equal to $2J + 1$ and for an occupied state it should be zero. The experimental values of 2.44(20) for the $3/2^-$ ground state and 1.36(16) for the $7/2^-$ level at 1740(95) keV show that neutrons start moving from $\nu f_{7/2}$ to $\nu p_{3/2}$ in ^{46}Ar. About 80% of the $\nu p_{1/2}$ and 65% of the $\nu f_{5/2}$ strength was observed. The shell-model calculations have been relied upon to reconstruct the missing strength and extract the single-particle energies. We can derive a weakening of the νf and νp spin-orbit splittings between ^{49}Ca and ^{47}Ar by 875 keV and 207 keV, respectively. If we impute this to the removal of two protons from the nearly degenerate $\pi d_{3/2}$ and $\pi s_{1/2}$ orbitals, then it is the tensor interaction through the $\pi d_{3/2}$ particles and density-dependent forces particularly for $\pi s_{1/2}$ that can be held responsible.

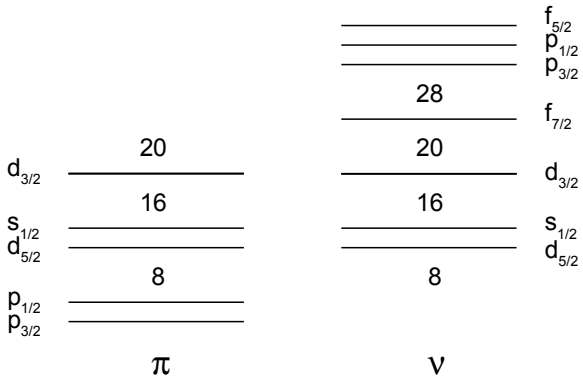

Fig. 1. Aide-mémoire of the shell-model orbitals discussed in the text.

3. Conclusions

Experimental results around the $Z = 14$, $N = 14, 16$ and 28 shell gaps or subshell gaps that were obtained at Ganil over the last years have been presented in this paper. The neutron–neutron and proton-neutron interactions modulate the strength of these gaps in a way that depends on the specific valence orbitals at play. The resulting displacements of shell gaps are all the more unexplored if one ventures farther out of stability. While the two-body matrix elements of shell-model interactions implicitly contain the ingredients of these displacements, it is not always easy to trace their precise origin. Here we offer a first-order interpretation in which the spin-orbit force is seen to compete with the tensor force. A more detailed account of the evolution of magic numbers far from stability can be found in Ref. [17].

If the tensor force is pervasive throughout the nuclear chart then the valence orbitals in ^{20}C, being $\pi p_{3/2}$ and $\nu d_{5/2}$, are mutually repulsive. The latter state is pushed upwards and a $N = 14$ subshell gap cannot develop, unlike in the oxygen isotopes. Mirror symmetry in ^{36}Ca would call for a repetition of what happens in ^{36}S before entering the island of inversion. For ^{36}Ca, is it the filled $\pi d_{3/2}$ state that repels $\nu d_{3/2}$ but attracts $\nu d_{5/2}$, opening $N = 16$ and lending to this isotope a magic character (the $\nu s_{1/2}$ particles do not feel the tensor force [18]). The same principle acts once again in an opposite way when the repulsion between $\pi d_{5/2}$ and $\nu f_{7/2}$ in ^{42}Si reduces the $Z = 14$ and $N = 28$ gaps, provoking the development of oblate deformation. For ^{47}Ar the picture is somewhat more subtle. Starting our description from ^{49}Ca, the removal of protons lessens the tensor attraction between $\pi d_{3/2}$ and $\nu f_{7/2}$ in ^{47}Ar. Superimposed on this, the partial depletion of $\pi s_{1/2}$ creates a modified density distribution in the interior of the nucleus that affects the spin-orbit splitting in particular of the νp orbitals. The net effect is a decrease of the $N = 28$ gap.

An important caveat is that the orbital filling in the preceding picture may be too simplified: it is only meant to be qualitative. Also, calculations with different shell-model and mean-field codes may also be able to account for the observed effects without invoking the typical tensor-force behaviour of repulsion and attraction between states with aligned or anti-aligned angular momentum, respectively.

REFERENCES

[1] J. Dobaczewski *et al., Phys. Rev. Lett.* **72**, 981 (1994).
[2] T. Otsuka *et al., Phys. Rev. Lett.* **97**, 162501 (2006).
[3] M. Stanoiu *et al., Phys. Rev.* **C78**, 034315 (2008).
[4] L. Fifield *et al., Nucl. Phys.* **A385**, 505 (1982).

[5] M. Stanoiu *et al., Phys. Rev.* **C69**, 034312 (2004).
[6] I. Talmi, I. Unna, *Phys. Rev. Lett.* **4**, 469 (1960).
[7] A. Bürger *et al.*, to be published.
[8] P. Doornenbal *et al., Phys. Lett.* **B647**, 237 (2007).
[9] G. Audi, A. Wapstra, C. Thibault, *Nucl. Phys.* **A729**, 337 (2003).
[10] J.P. Dufour *et al., Z. Phys.* **A324**, 487 (1986).
[11] A. Gade *et al., Phys. Rev.* **C77**, 044306 (2008).
[12] B. Bastin *et al., Phys. Rev. Lett.* **99**, 022503 (2007).
[13] C. Campbell *et al., Phys. Rev. Lett.* **97**, 112501 (2006).
[14] E. Caurier *et al., Nucl. Phys.* **A742**, 14 (2004).
[15] L. Gaudefroy *et al., Phys. Rev. Lett.* **97**, 092501 (2006).
[16] S. Nummela *et al., Phys. Rev.* **C63**, 044316 (2001).
[17] O. Sorlin, M.-G. Porquet, *Prog. Part. Nucl. Phys.* **61**, 602 (2008).
[18] T. Otsuka *et al., Phys. Rev. Lett.* **95**, 232502 (2005).